

Experimental Evidence for a Highly Reversible Excited State Equilibrium between *s*-Cis and *s*-Trans Rotational Isomers of 2-Methoxynaphthalene in Solution

Ioanna Balomenou and George Pistolis*

Contribution from the NCSR "Demokritos" Institute of Physical Chemistry,
153 10 Athens, Greece

Received June 25, 2007; E-mail: pistolis@chem.demokritos.gr

Abstract: Detailed studies on the kinetics and the thermodynamics of the excited-state torsional isomerization of the title molecule (**1**) relative to exocyclic C2–O bond, when dissolved in 3-methylpentane, are reported by means of nontime- and time-resolved fluorescence spectroscopy. Over the broad temperature range studied, **1** exists in spectrally distinct, thermally equilibrated *s*-cis and *s*-trans conformations in the ground state (S_0). In the lowest excited singlet state (S_1) and above 260 K a pure adiabatic interconversion channel is activated that interconverts *s*-cis* and *s*-trans* conformers through a nearly fully reversible isomerization pathway with an activation energy of about 29 kJ/mol. The excited-state equilibrium constant is found to be remarkably temperature-independent just barely exceeding 1 above 260 K. Contrary to the predominantly irreversible photoisomerization mechanism generally observed in related compounds, this work provides insights into the high reversibility of an excited-state rotameric equilibration in solution.

1. Introduction

Rotational isomerism in the *excited state* is a photochemical mechanism which interconverts *s*-cis* and *s*-trans* conformers during their lifetime, upon rotation about the single bond that joins a suitable conjugated group to an aromatic moiety (Aryl–C=).^{1–7} Manifestation of the rotational isomerization in the singlet excited state of 2-vinyl-anthracene (2VA) and its α - or β , β' -dialkyl derivatives was originally reported from Barbara and co-workers,¹ and later 2VA was reinvestigated by others.² Thereafter the above photodynamic scheme was demonstrated in similar systems including 3,3'-dimethylstilbene,³ 2-anthryl-ethylenes,⁴ *N*-methoxy-1-(2-anthryl)ethanimine derivatives,⁵ and 1,3-di-(3'-thienylethenyl)benzene.⁶ The one-way photochemical adiabatic isomerization of aromatic olefins has also been comprehensively reviewed by Arai and Tokumaru.⁷

It is generally accepted that the above torsional photoisomerization process proceeds one way^{2,4–7} (*forward*), from the higher to the lower energy rotamer; the opposite way (*reverse*), if existing, is not significant and has no substantial affect on the

observable thermal activation parameters.¹ Very recently the above photodynamic scheme was demonstrated mainly experimentally for 2-methoxyanthracene and some of its derivatives in solution.⁸ In the above work it is proposed that one-way interconversion from the *s*-cis* into the *s*-trans* conformations, within their singlet excited-state lifetimes, takes place.⁸ The *s*-cis and *s*-trans configuration are assigned according to the orientation of the methoxy group relative to the long axis of the anthracene subunit. However, the absence of pure rotameric spectroscopic analysis and the lack of accurate theoretical methods to date, capable of reliably handling the sizable electronic features of 2-methoxyanthracene and its derivatives,⁸ prevent an in-depth kinetic analysis for these compounds. On the contrary, the simpler analogue 2-methoxynaphthalene (**1**) has been extensively studied by jet-cooling spectroscopy and ab initio calculations,⁹ although so far it is unexplored in the condensed phase. We now report mainly on the excited-state dynamics of rotameric interconversion of **1**, addressing specifically the issue of possible new kinetic manifestations on torsional isomerization in solution. The general scheme of our investigations is given below.

2. Experimental Section

2.1. Materials: 2-Methoxynaphthalene (**1**) was purchased from Fluka and was first purified by vacuum sublimation and then by recrystallization from a mixture of methanol and chloroform. 3-Methylpentane

- (1) (a) Brearley, A. M.; Stanjord, A. J. G.; Flom, S. R.; Barbara, P. F. *Chem. Phys. Lett.* **1985**, *113*, 43. (b) Flom, S. R.; Nagajan, V.; Barbara, P. F. *J. Phys. Chem.* **1986**, *90*, 2085–2092. (c) Brearley, A. M.; Flom, S. R.; Nagajan, V.; Barbara, P. F. *J. Phys. Chem.* **1986**, *90*, 2092–2099. (d) Barbara, P. F.; Janeba, W. *Acc. Chem. Res.* **1988**, *21*, 195.
- (2) Arai, T.; Karatsu, T.; Sakuraki, H.; Tokumaru, K.; Tamai, N.; Yamazaki, I. *Chem. Phys. Lett.* **1989**, *158*, 429.
- (3) Park, N. S.; Waldeck, D. H. *Chem. Phys. Lett.* **1990**, *168*, 379.
- (4) Karatsu, K.; Itoh, H.; Yoshikawa, N.; Kitamura, A.; Tokumaru, K. *Bull. Chem. Soc. Jpn.* **1999**, *72*, 1837.
- (5) Furuuchi, H.; Arai, T.; Sakuragi, H.; Tokumaru, K.; Nishimura, Y.; Yamazaki, I. *J. Phys. Chem.* **1991**, *95*, 10322–10325.
- (6) Bartocci, G.; Ginocchietti, G.; Mazzucato, U.; Spalletti, A. *Chem. Phys.* **2006**, *328*, 275.
- (7) Arai, T.; Tokumaru, K. *Chem. Rev.* **1993**, *93*, 23.

- (8) Albrecht, M.; Bohne, C.; Granzhan, A.; Ihmels, H.; Pace, T. C. S.; Schnurpfeil, A.; Waidelich, M.; Yihwa, C. *J. Phys. Chem. A* **2007**, *111*, 1036.
- (9) (a) Troxler, T.; Pryor, B. A.; Topp, M. R. *Chem. Phys. Lett.* **1997**, *274*, 71. (b) Troxler, T. *J. Phys. Chem. A* **1998**, *102*, 4775. (c) Johnson, J. R.; Jordan, K. D.; Plusquellic, D. F.; Pratt, D. W. *J. Chem. Phys.* **1990**, *93*, 2258.

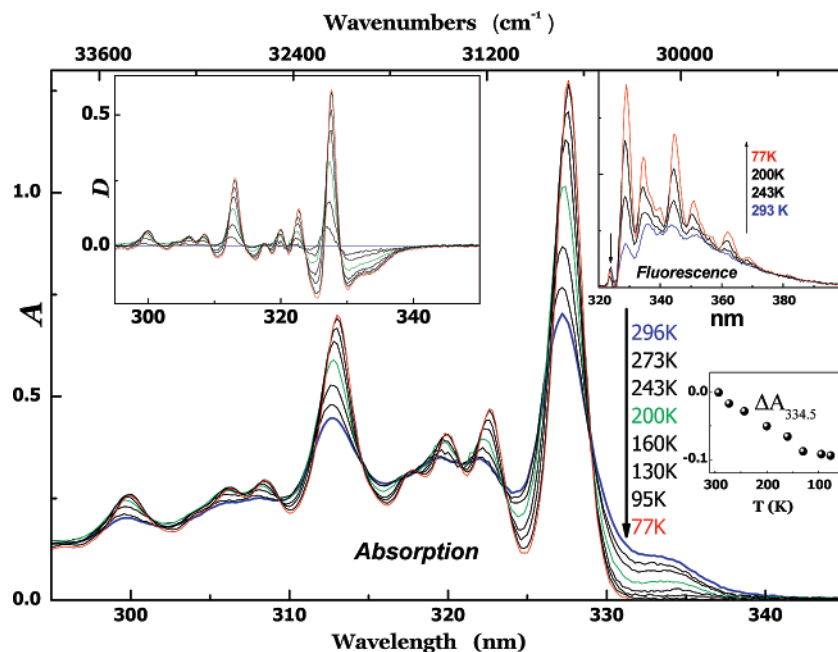


Figure 1. Absorption spectra of **1** in 3-MP (2×10^{-4} M) at varying temperatures: (Insert left top) Difference spectra ($T - 296$). Isosbestic points observed at 329, 323.6, 320.8, 318, 314.6, and 309.4 nm. The spectra have been corrected for temperature dependence of the density of the solution; (right top insert) fluorescence spectra of **1** in 3MP (3.26×10^{-5} M) at varying temperatures excited selectively at 323.6 ± 0.1 nm (isosbestic point). Wavelength resolution of the fluorescence is 1 nm. Spectra have been corrected for the nonlinearity of the instrument response. The arrow indicates the peak due to scattered excitation light. (Insert right bottom) Absorption changes at 334.5 nm vs T .

(3MP) was filtered through a water-cooled chromatographic column packed with a combination of silica gel (activity grade I) in the lower half and basic alumina (super active) in the upper half. Finally, it was distilled in a glass-filled column under an argon atmosphere.

2.2. Instrumentation and Methods: Absorption spectra were recorded on a Perkin-Elmer Lambda-16 spectrophotometer. Steady-state fluorescence spectra were accomplished by the Perkin-Elmer model LS-50B and the Edinburgh Instruments model FS-900 spectrofluorometer. Fluorescence lifetimes (τ) were determined using the time-correlated single-photon counter FL900, of the above Edinburgh Instruments setup, which is capable of measuring lifetimes down to 100 ps. For measurements at ambient temperatures, the samples were degassed by using the freeze–pump–thaw technique six or more times. For low-temperature experiments samples were degassed by bubbling nitrogen (99.9999%). As standard a reference for quantum yield determinations, we utilized a solution of quinine sulfate in 0.1 N H_2SO_4 ($\Phi_s = 0.54 \pm 0.02$).¹⁰ Samples above 6 °C were thermostated to ± 0.1 °C using a circulating water bath. For low-temperature measurements, a sealed cryogenic rectangular quartz cuvette was enclosed in a copper block mounted on the coldfinger of a liquid nitrogen cryostat (Oxford Instruments, PE1704). All the experiments were accomplished under a helium atmosphere. Special care was taken to ensure that the glass formed by the frozen solvent was not cracked. To avoid any deviation in spectral analysis, we subtracted the solvent's spectra from the samples, at every temperature. The dependence of density (ρ) on temperature (T) was corrected by using a third-order polynomial:¹¹ $\rho(T) = B_0 + B_1T + B_2T^2 + B_3T^3$; (B_0 ; B_1 ; B_2 ; B_3) = ($9.273\ 80 \times 10^{-1}$; $-1.059\ 10 \times 10^{-3}$; $1.091\ 70 \times 10^{-6}$; $-1.841\ 90 \times 10^{-9}$) for 3MP. The temperature dependence of the solvent index of refraction (n) was calculated from standard methods.¹²

All computer fits and simulations, except those of time-resolved experiments, were performed using the program "Micro Math Scientist for Windows", version 2.01, of Micro Math.

Table 1. Fluorescence Quantum Yields (Φ), Lifetimes (τ), Radiative (k_f) and Nonradiative Rates Constants (k_{nr}), Absorption ν_{0-0}^a and Fluorescence ν'_{0-0} Transitions Origins of A and B Rotameric Isomers of **1** Obtained at Low Temperatures

rotamer	Φ^c	τ (ns) ^d	$k_f \times 10^7$ (s ⁻¹) ^d	$k_{nr} \times 10^7$ (s ⁻¹) ^d	ν_{0-0}^a (cm ⁻¹)	ν'_{0-0} (cm ⁻¹)
A ^a	0.72	13.0	5.54	2.15	30 525	30 583
B ^b	0.68	13.0	5.23	2.46	29 895	29 980

^a "Limiting" values ≤ 130 K. ^b Obtained at 160 K. ^c Uncertainties in low-temperature quantum yields $< 8\%$. ^d Uncertainties in recovered lifetimes and rates $< 5\%$ and $< 8\%$, respectively.

3. Results and Discussion

3.1. Spectroscopy below 260 K. Figure 1 displays the temperature dependence of the absorption spectrum of **1** dissolved in 3MP, upon cooling stepwise from 296 to 77 K. As clearly shown the weak absorption band (~ 333 nm) gradually disappears whereas several isosbestic points emerge across the absorption spectrum. The above features strongly suggest the existence, in the ground state, of two discrete forms A and B of **1** in thermal equilibrium. Additionally, aggregation phenomena do not seem to be present on freezing to the glass transition temperature of 3MP (~ 77 K). Furthermore the absorption spectrum shows no appreciable changes with temperature below 130 K demonstrating that it is due entirely to the more stable form A (see also Figure 1, right bottom insert).

The fluorescence spectra, on the other hand, also show quite remarkable characteristics (Figure 1 right top insert). When the sample is preferentially excited at an isosbestic point of the absorption band, the total integrated fluorescence intensity increases with decreasing temperature indicating an augmentation of the absolute quantum yield from 0.36 ± 0.02 at ambient temperatures to 0.7 ± 0.04 below 130 K (see also Figure 2; Table 1). Furthermore, the relative intensity mainly of the "0–0" emission peak is strongly temperature dependent and

(10) Demas, J. N.; Crosby, G. A. *J. Phys. Chem.* **1971**, *75*, 991.

(11) Ruth, A. A.; Nickel, B.; Lesche, H. Z. *Phys. Chem.* **1992**, *175*, 91.

(12) Riddick, J. A.; Bunger, W. B.; Sakano, T. K. *Organic Solvents*; John Wiley & Sons: 1986.

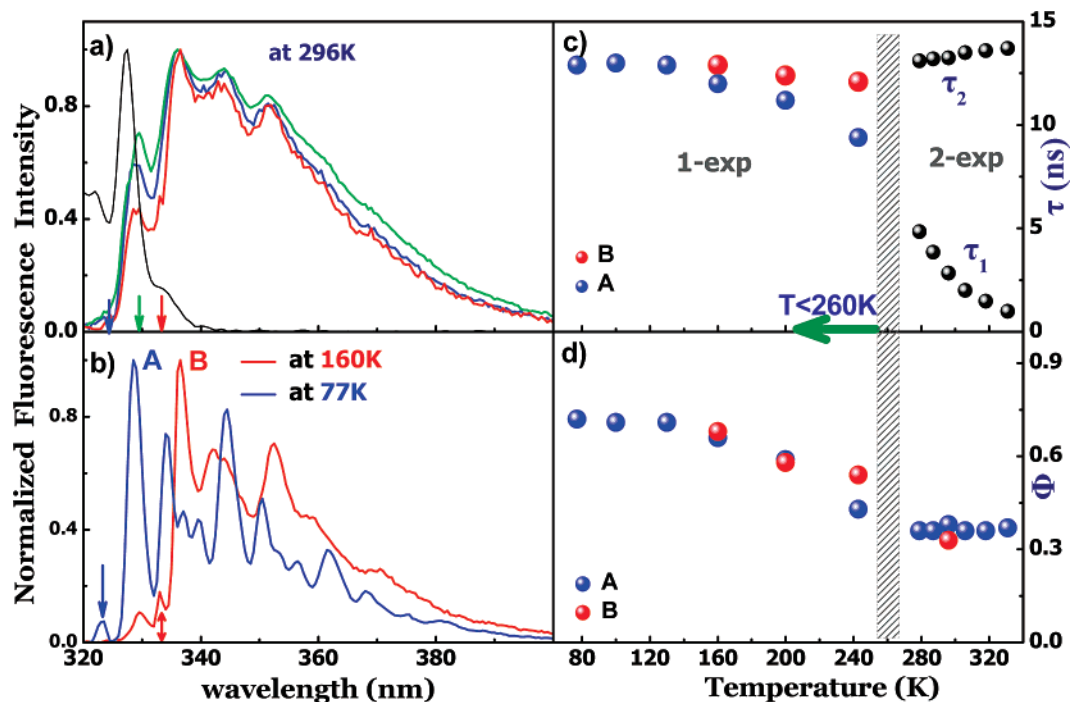


Figure 2. Normalized absorption-fluorescence spectra, quantum yields, and lifetimes of **1** in 3MP. (a) Absorption spectrum (left) and fluorescence spectra (right) excited selectively (see arrows for $\lambda_{\text{exc}} \pm 0.1$ nm), at room temperature; scattered excitation light has been removed. (b) Pure emission spectra of A* and B* rotamers. Emission of A* is obtained at 77 K in a dilute solution of $\sim 3 \times 10^{-5}$ M. For pure B* emission a solution of $\sim 2 \times 10^{-4}$ M at 160 K was used (see arrows for $\lambda_{\text{exc}} \pm 0.1$ nm). (c) Lifetimes of A* and B*; excitation and emission observation wavelength (exc/em) were, respectively, $322 \pm 5/328 \pm 2$ nm for A* and $335 \pm 2/345 \pm 7$ nm for B* below 260 K. Above 260 K coupled biexponential kinetics was observed (see part B). (d) Absolute quantum yields (Φ) at varying temperatures corrected for refractive index variation with temperature (excitation wavelengths as in Figure 2b).

increases sharply, by analogy to the “0–0” absorption transition, with decreasing temperature. After analysis of the above experimental data we find that the reason for the increase of quantum yield is a consequence of an increase of the radiative rate constant ($k_{f,A}$) of the A* emitting species.¹³ The fluorescence spectra of **1** below ~ 130 K, likewise to the absorption spectra at these temperatures, have no appreciable changes. This latter observation provides additional evidence that practically the spectrum of **1** is due entirely to the more stable form A at low temperatures.

Below 260 K the barrier controlled isomerization rate, in the excited state, is much slower than the fluorescence decay, that is, $k_1 + k_{-1} \ll k_A$. As a consequence, A* and B* do not

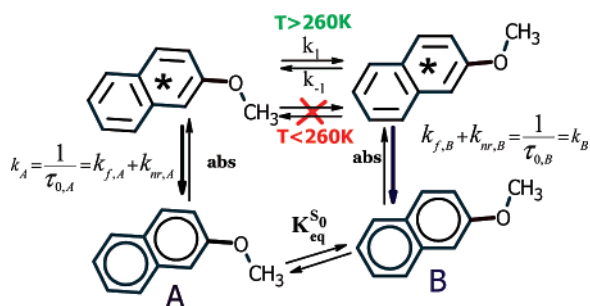
interconvert during their lifetime and decay independently according to the so-called NEER (nonequilibrium of excited rotamers) rule.¹⁴ Therefore, direct excitation at an appropriate wavelength in which B absorbs solely will give pure B* emission. Indeed, the dramatic photoselection observed with excitation at $\lambda \geq 333$ nm (Figure 2b) provides further evidence that there is an additional species B in the ground state which is thermodynamically less stable and absorbs at longer wavelengths than the dominant one (A). The pure spectra of A can be easily obtained below 130 K. As becomes evident from the above spectroscopic analysis, the high-energy part (329 ± 3 nm) of the fluorescence spectrum shown in Figure 2a contains no contribution from B* emission and therefore is a signature of the emission of the A* rotamer only (see also Figure 2b). Consequently, this wavelength region can serve for monitoring fluorescence decay traces of pure A* at any temperature. The absolute quantum yields and the recovered fluorescence lifetimes as a function of temperature for both emitting species are also given in Figure 2c,d. For both emitting species A* and B* below 260 K, the fluorescence intensity versus time can be fitted very successfully with a single-exponential function. The results clearly show the following: (1) the “limiting” quantum yields of the A* and B* rotamer respectively are, within experimental uncertainty ($< 8\%$) closely identical, namely, $\Phi_{0,A} = 0.72$ and $\Phi_{0,B} = 0.68$, and (2) they have indistinguishable lifetimes below 160 K ($\tau_{0,A} = \tau_{0,B} = 13.0 \pm 0.2$ ns). The most important photophysical parameters are summarized in Table 1.

3.1.1. Assignment of A and B Rotamers: The “0–0” electronic transition of the high-energy rotamer A of **1** in 3MP

(13) The remarkable increase of the molar extinction coefficient (ϵ_{max} , $\lambda \sim 327$ nm), upon lowering the temperature, suggests that the radiative transition probability should be increased according to the well-known relation between the fluorescence and absorption properties of organic molecules (see for example: Strickler, S. J.; Berg, R. A. *J. Chem. Phys.* **1962**, *37*, 814). The increase of ϵ_{max} by a factor of ~ 2 , from ambient to low temperatures, is consistent with the ratio of the experimentally measured quantum yields at these temperatures ($\Phi^{77}/\Phi^{296} \cong 0.7/0.36 \cong 2$). On the basis of our experimental findings that the rate constant of the destruction of S₁ ($1/\tau_0 \cong 13^{-1}$ ns⁻¹ for both rotamers) at low temperatures (see Table 1) is equal to the nonisomerization rate constant ($k_A = k_{f,A} + k_{nr,A} = 1/\tau_2 \approx 1/13.3$ ns⁻¹) above 260 K (see Table 2), it is concluded that Φ 's values are primarily driven by the radiative rate constant (k_f). The decrease of the radiative transition probability as temperature rises (and, in turn, the hydrocarbon matrix softens) is most likely due to the presence of conformationally distorted populations of the A form of **1**, in which the methoxy torsion angle deviates slightly from its equilibrium position ($\varphi = 0^\circ$, *s*-*cis* configuration). Based on the results obtained for *cis*-**1**^{9b} and *cis*-2-hydroxynaphthalene^{9c} where it has been clearly shown that the σ/π mixing between the oxygen lone pair and the naphthalene orbitals determines the transition dipole moment orientation, it seems plausible to suggest that the methoxy torsion angle should significantly affect the degree of coupling between orbitals of the oxygen and naphthalene subunit and accordingly the transition moment and the oscillator strength. The above are also suggested with results obtained at cryogenic temperatures (4.2 K) where we found that the degree of inhomogeneity upon the excitation and emission spectra of **1** is not significant.¹⁵

(14) For a review see: Jacobs, H. J.; Havinga, E. *Adv. Photochem.* **1979**, *11*, 305–373. See also: Mazzucato, U.; Momiccioli, F. *Chem. Rev.* **1991**, *91*, 1679.

Scheme 1



occurs at $30\,525\text{ cm}^{-1}$ (327.6 nm) and is close to that observed in jet-cooled **1**^{9a} ($31\,028\text{ cm}^{-1}$). Furthermore, the separation of the S_1 – S_0 electronic origin transitions of the A and B rotameric forms of **1** observed in the present work (630 cm^{-1}) nearly coincides with the one obtained from the jet-spectra of **1**⁹ (660 cm^{-1}). The above configurations A and B have been assigned respectively to a *cis* (*syn*, $\varphi = 0^\circ$) and a *trans* (*anti*, $\varphi = 180^\circ$) conformation.^{9a,b} The *syn* and *anti* are denoted by the dihedral angle $\varphi(\text{C}_1\text{--C}_2\text{--O}_{11}\text{--C}_{12})$ of the methoxy group relative to the naphthalene plane. Our analysis on the fluorescence and fluorescence excitation spectral vibronic features at cryogenic temperatures (4.2 K) also suggest the *s-cis* configuration.¹⁵ A crystallographic analysis at 173 K proves that **1** crystallizes as a nearly planar molecule with the methoxy group adopting a *syn*-periplanar conformation with respect to the C_1 atom.¹⁶ Finally, from ^1H and ^{13}C nuclear magnetic resonance experiments of **1** in carbon tetrachloride solutions, a conformational preference of the *cis*- over the *trans*-configuration is found;¹⁷ quantitative analysis led to an approximate population ratio of 19:1 between *cis* and *trans* rotameric isomers at 305 K .¹⁷ We therefore assign the A form as the *s-cis* rotamer which isomerizes to the *s-trans* analogue as temperature increases. The equilibrium constant for S_0 ($K_{\text{eq}}^{S_0} = [\text{B}]/[\text{A}]$) is estimated to be ~ 0.07 at 296 K from the absorption spectra.^{1b} This estimate corresponds to a $\Delta H^{S_0} \approx 6.5\text{ kJ/mol}$ ($\sim 550\text{ cm}^{-1}$). For comparison a value of ~ 0.05 for **1** in carbon tetrachloride can be estimated (see above). A value of ~ 0.1 for the analogues rotamers of 2-vinylanthracene in cyclohexane has also been reported.^{1b}

3.2. Spectroscopy above 260 K. Above 260 K a pure adiabatic interconversion channel in the excited state between A^* and B^* rotamers is switched on, as manifested by dynamic fluorescence analysis (vide infra). **1** follows the fluorescence kinetics commonly observed in analogous systems.¹ Briefly, coupled biexponential kinetics with a short (τ_1) and a long (τ_2) lifetime component showing no wavelength dependence, was observed.

$$I(t, \lambda) = A_1(\lambda) \exp(-t/\tau_1) + A_2(\lambda) \exp(-t/\tau_2) \quad (1)$$

At the high-energy part of the fluorescence spectrum, both A_1 and A_2 are positive. When decay traces are detected at emission wavelengths where the B^* (*s-trans*) rotamer considerably emits, A_1 becomes negative demonstrating *s-cis** and *s-trans** rotameric interconversion.

For a given *hypothetical adiabatic* photodynamic model, as in Scheme 1, if the *nonisomerization* rate constants $k_A = 1/\tau_{0,A}$

and $k_B = 1/\tau_{0,B}$ are equal then the solution of the coupled differential equations for the A^* and B^* deactivating processes leads explicitly to the simple but very important relations^{1b}

$$\tau_2^{-1} = \tau_{0,B}^{-1} \quad (2)$$

and

$$\tau_1^{-1} - \tau_2^{-1} = k_1 + k_{-1} = k_{\text{sum}} \quad (3)$$

Analysis of the time-resolved fluorescence decay traces indicates the following (see Table 1): (1) τ_2 remains exceptionally independent of temperature and within experimental error is equal to $\tau_{0,B} \cong \tau_{0,A} \cong 13.3\text{ ns}$ obtained at low temperatures; this provides additional evidence with respect to the adiabaticity of the isomerization and the equality of the nonisomerization rate constants ($k_A \cong k_B$).¹³ (2) The fluorescence decay traces, selected at a narrow wavelength region signed by the emission of the A^* rotamer only ($328 \pm 2.0\text{ nm}$) (Figure 2b), can be strictly fitted to a biexponential function; this is also a signature for the reversibility of the excited-state reaction,¹⁸ and (3) the amplitude ratio A_2/A_1 is nontemperature dependent and close to 1 (see also Figure 3a; insert). From the decay times τ_1 and τ_2 and the amplitude ratio A_2/A_1 together with the “limiting” lifetime $\tau_{0,A}$, the *forward* rate constant k_1 can be unambiguously determined;¹⁹ k_{-1} is then obtained from k_{sum} . In fact, the above procedure should be slightly corrected for the fraction of the initially excited $[\text{B}_0]^*$ resulting from direct excitation of the ground state population of the B (*s-trans*) isomer.²⁰

3.2.1. Energy Barriers, Thermodynamics, and Reaction Coordinate. From the recovered rate constants in an Arrhenius analysis (Figure 3a and Table 2), the S_1 thermal activation parameters can be evaluated. If the *forward* and *reverse* reaction were, in principle, to have different activation energies E_a^1 and E_a^{-1} , respectively, then $\ln k_{\text{sum}}$ vs $1/T$ would be nonlinear because k_{sum} , in fact, follows a biexponential form (eq 4).

$$k_{\text{sum}} = k_1^0 \exp(-E_a^1/RT) + k_{-1}^0 \exp(-E_a^{-1}/RT) \quad (4)$$

k_1^0 and k_{-1}^0 are Arrhenius frequency factors for the forward and reverse reaction, respectively. The unexpected linearity of $\ln k_{\text{sum}}$ (Figure 3a) can be explained only if either (a) the *forward* (k_1) and *reverse* (k_{-1}) reaction do have approximately indistinguishable energy barriers or (b) the *forward* predominates

(17) (a) Salman, S. R. *Spectrochim. Acta* **1984**, *40A*, 229. (b) Salman, S. R. *Magn. Reson. Chem.* **1985**, *23*, 119.

(18) (a) Lackowicz, J. R. *Principles of Fluorescence Spectroscopy*, 2nd ed.; Plenum Press: New York, 1999; p 519. (b) The fact that one sees double exponential behaviour of the A^* fluorescence decay traces is only part of the story. Further evidence concerning the presence of the *reverse* reaction (*s-cis** \leftrightarrow *s-trans**) comes directly from photoselection effects. An inspection of Figure 2 clearly shows that excitation at a wavelength in which *s-trans* (B) absorbs solely ($\lambda \geq 333\text{ nm}$) results in emission primarily from B below 260 K (Figure 2b). When temperature rises beyond the above temperature threshold a significant portion of A^* emission emerges (see Figure 2a). This suggests that a thermally activated isomerization process from the *s-trans** into the *s-cis** conformation takes place.

(19) Il'ichev, Y. V.; Kühnle, W.; Zachariasse, A. *J. Phys. Chem. A* **1998**, *102*, 5670.

(20) The general solution for the fluorescence intensity $I(t)$ of the A^* emitting species is given by the following: $I(t) = k_{f,A}\{(X - \beta_2)[\text{A}_0]^* - \kappa_{-1}[\text{B}_0]^*]/(\beta_1 - \beta_2)\} \exp(-\beta_1 t) + k_{f,A}\{(\beta_1 - X)[\text{A}_0]^* + \kappa_{-1}[\text{B}_0]^*\}/(\beta_1 - \beta_2)\} \exp(-\beta_2 t)$. $k_{f,A}$ is the radiative rate constant of A^* , X is the sum of the rates of all deactivation channels of A^* , $X = 1/\tau_{0,A} + k_1$, and β_1, β_2 are the measured rate constants, $1/\tau_1$ and $1/\tau_2$, respectively. From the ratio $A = A_2/A_1$ of the pre-exponential factors one obtains the following equation from which k_1 can be evaluated: $(1 + K_{\text{eq}}^{S_0})k_1 = 1/(1 + A)(1/\tau_1 - 1/\tau_{0,A}) + K_{\text{eq}}^{S_0} k_{\text{sum}}$. Notice that $K_{\text{eq}}^{S_0} = [\text{B}_0]^*/[\text{A}_0]^*$ and $\tau_2 = \tau_{0,B}$.

(15) Manuscript in preparation.

(16) Bolte, M.; Bauch, C. *Acta Crystallogr., Sect. C* **1998**, 1862.

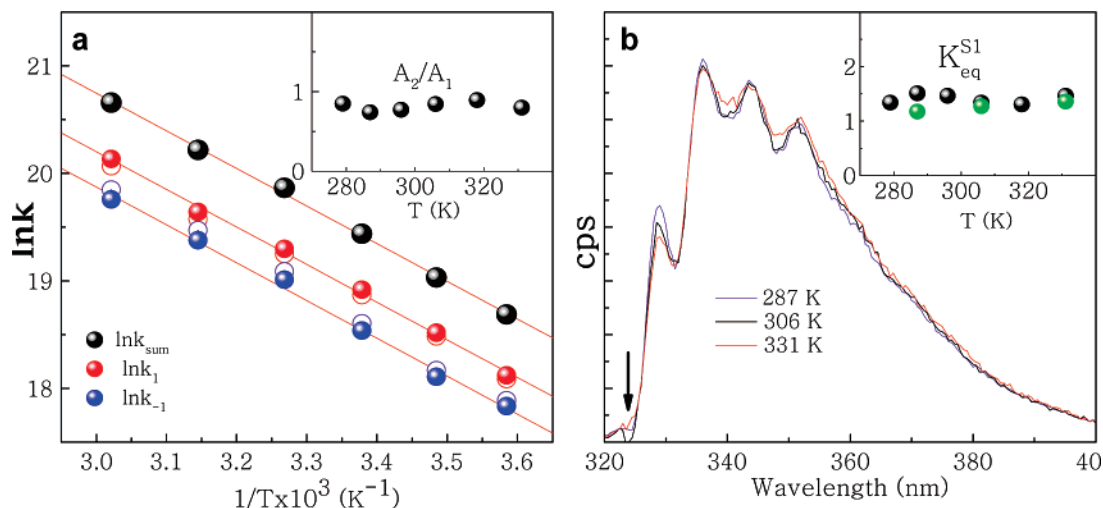


Figure 3. (a) An Arrhenius plot of k_{sum} , k_1 , and k_{-1} . Open and filled circles represent noncorrected and corrected values, respectively, for the presence of $K_{\text{eq}}^{\text{S}_1}(T)$. (Inset) Ratio of preexponential factors (A_2/A_1) vs T . (b) Original steady-state fluorescence spectra at varying T obtained with selective excitation at an isosbestic point (323.6 ± 0.1 nm). (Inset) Excited-state equilibrium constant $K_{\text{eq}}^{\text{S}_1}$ vs T estimated from dynamic (black circles) and static (green circles) fluorescence spectroscopy.

Table 2. Temperature Dependence of the Observed Lifetimes,^{a,b} Ratio of Preexponential Factors (A_2/A_1), and Recovered Rate Constants^b of **1** in 3-Methylpentane [**1**] = 5×10^{-5} M (Exc: 320 ± 5 nm; Em: 328 ± 2.0 nm)

T , K	τ_1 , ns	τ_2 , ns	$k_{\text{sum}} \times 10^8 \text{ s}^{-1}$	(A_2/A_1)	$k_1 \times 10^8 \text{ s}^{-1}$	$k_{-1} \times 10^8 \text{ s}^{-1}$
279	4.84	13.12	1.30	0.85	0.74	0.55
287	3.85	13.20	1.84	0.74	1.10	0.73
296	2.84	13.24	2.77	0.77	1.64	1.12
306	2.01	13.50	4.23	0.84	2.40	1.80
318	1.48	13.60	6.02	0.89	3.39	2.60
331	0.99	13.70	9.34	0.80	5.54	3.80

^a The statistical parameter χ^2 was between 1.00 and 1.07. ^b Uncertainties in lifetimes and $k_{\text{sum}} < 5\%$; uncertainties in preexponential factors and recovered rates $< 10\%$.

significantly over the *reverse*,^{1b} that is, the isomerization reaction is in fact predominantly irreversible ($k_{\text{sum}} \approx k_1$). An Arrhenius analysis of the k_{sum} and the individual k_1 and k_{-1} gives respectively $E_a^{\text{sum}} = 29.1$ kJ/mol, $E_a^1 = 29.0$ kJ/mol, and $E_a^{-1} = 29.3$ kJ/mol which are actually indistinguishable. An insignificant variation within $\sim 3\%$ was found when the corresponding noncorrected values, for the presence of the ground state equilibrium $K_{\text{eq}}^{\text{S}_1}(T)$, were employed. It should be noted that three independent sets of experiments were carried out to determine the uncertainty associated with each point. We were unable to observe differences in rate constants and energy barriers exceeding remarkably the experimental error ($\leq 10\%$).

Besides the dynamic fluorescence spectroscopy findings, we have also made an indirect determination of the excited-state isomerization kinetics from static quantum yield measurements. We found that above 260 K the overall fluorescence quantum yield $\bar{\Phi}$ of a dilute solution of **1** in 3MP is completely independent from both temperature and wavelength of excitation, within experimental uncertainty ($\bar{\Phi} = 0.36 \pm 0.02$)²¹ (see also Figure 2d, $T > 260$ K). On the basis of the above and previous findings in part A, it is easy to show that the ratio of the individual quantum yields of the *s-trans** (B^*) and *s-cis** (A^*) species is given by²¹

$$\Phi_B/\Phi_A \approx K_{\text{eq}}^{\text{S}_1} \quad (5)$$

Interestingly, as seen in Figure 3b, the effect of temperature on the steady-state fluorescence spectra, after excitation at an isosbestic point (323.6 ± 0.1 nm), is actually insignificant. After detailed analysis of the above spectra, we find the following: (a) From the ratio of fluorescence intensities at the origin emission maxima 329 (A^*) and 336 nm (B^*) (pure B^* intensity was retrieved by subtracting the portion of A^* emission at 336 nm according to the pure rotameric spectral analysis made before; see Figure 2b), one obtains²¹ $K_{\text{eq}}^{\text{S}_1}$ values of 1.17, 1.27, and 1.36 at 287, 306, and 331 K, respectively; these values just barely exceed 1 and are in excellent agreement with those recovered from dynamic fluorescence kinetic analysis ($K_{\text{eq}}^{\text{S}_1} = k_1/k_{-1}$) (see Figure 3b; inset). (b) The absence of a significant temperature effect on Φ_B/Φ_A , that is $K_{\text{eq}}^{\text{S}_1}$, conclusively implies that the forward (E_a^1) and reverse (E_a^{-1}) activation energies should be approximately equal. In other words, our steady-state experiments, in extraordinary agreement with dynamic fluorescence analysis, suggest a nearly fully reversible isomerization path in S_1 above 260 K. If one were to have one-way or a predominant isomerization from the 1-*cis** into 1-*trans** configuration path, that is $k_{\text{sum}} \approx k_1$, then one would expect Φ_B/Φ_A to increase dramatically as the temperature rises.²²

The above suggest that for the present interconversion process, both the standard (ΔH^{S_1}) and the free reaction enthalpy ($\Delta G_{(T)}^{\text{S}_1}$, for $T > 260$ K) should be very close to 0.²³ From the Arrhenius frequency factors for the forward (k_1^0) and reverse

- (21) For a photodynamic model given in scheme 1, upon continuous illumination the rate of construction of each emitting species A^* and B^* is equal to its rate of deconstruction according to the following relations: $0 = d[A^*]/dt = -(k_A + k_1)[A^*] + k_{-1}[B^*] + I_A$ and $0 = d[B^*]/dt = -(k_B + k_{-1})[B^*] + k_1[A^*] + I_B$. k_A and k_B represent the nonisomerization rates constants ($1/\tau_{0,i}$, $i = A$ or B), and I_A and I_B are the rates of absorption of photons by A and B , respectively. The quantum yield for each species can be expressed as follows: $\Phi_A = k_{f,A}/(k_A + k_B K_{\text{eq}}^{\text{S}_1})$ and $\Phi_B = k_{f,B} K_{\text{eq}}^{\text{S}_1}/(k_A + k_B K_{\text{eq}}^{\text{S}_1})$ where $K_{\text{eq}}^{\text{S}_1} = [B^*]/[A^*]$. From the equality of the nonisomerization rates $k_A \approx k_B \approx 1/13.3 \text{ ns}^{-1}$ and the temperature/wavelength independence of the total quantum yield Φ , it is concluded that A^* and B^* rotamers should have identical radiative rates constants ($k_{f,A} = k_{f,B} = \Phi \times k_A = 2.70 \times 10^7 \text{ s}^{-1}$) above 260 K (see also ref 13). Therefore one obtains $\Phi_B/\Phi_A \approx K_{\text{eq}}^{\text{S}_1}$.
- (22) See for example: (a) Maus, M.; Rettig, W. *J. Phys. Chem.* **2002**, *106*, 2104. (b) Yoshihara, T.; Druzhinin, S. I.; Zachariasse, K. A. *J. Am. Chem. Soc.* **2004**, *126*, 8535.

(k_{-1}^0) reaction the isomerization reaction entropy, ΔS^{S_1} , is estimated to be $\cong 2 \text{ J}\cdot\text{K}^{-1}\cdot\text{mol}^{-1}$. A second estimation of ΔH^{S_1} can be made from the energy separation of the absorption maxima of the A and B rotamers and their ground state ΔH^{S_0} , namely, $\Delta H^{\text{S}_1} = \Delta E_{\text{A-B}} - \Delta H^{\text{S}_0}$; this procedure roughly gives $\sim 0.8 \text{ kJ/mol}$ supporting the kinetic results.

Most importantly, the results indicate that the torsional motion (φ) (about the bond that joins the methoxy group to the aromatic moiety) between interconvertible the *cis* ($\varphi = 0^\circ$) and *trans* ($\varphi = 180^\circ$) configuration of **1** must have taken place nearly isoenergetically through an almost fully symmetrical effective torsional potential of the form^{1b} $2V(\varphi) \cong E_a^1(1 - \cos 2\varphi)$. Although detailed electronic structures and accurate energies of both configurations of **1** in S_1 (*s-cis** and *s-trans**) are not yet supported by theoretical methods, however, extensive ab initio calculation by Troxler^{9b} of the *s-cis* form of **1** revealed that the oxygen atom considerably exhibits sp^2 character in both electronic states. In the S_1 state the sp^2 character is larger,^{9b} and therefore resonance interactions, between planarized oxygen atom of the methoxy group and aromatic moiety, are expected to be more favorable (see also next paragraph). As a result the methoxy group of **1** isomerizes in a relatively similar way to a conjugated group (comparable in size to the methoxy group) joined to an aromatic ring, for example, 2-vinylnaphthalene (2VA).^{1b} This suggestion is further corroborated quantitatively by the fact that the activation energies for the *s-cis** \leftrightarrow *s-trans** interconversion ($\sim 29 \text{ kJ/mol}$) obtained in the present work are in reasonable agreement with those reported for the *forward* (22.2 kJ/mol) and the *reverse* (28.9 kJ/mol) isomerization reaction of 2VA^{1b} in cyclohexane. For the more closely structurally related 2-methoxyanthracene a value of 19 kJ/mol for the one-way (*forward*) rotational barrier of the methoxy group has been reported.⁸ This value differs remarkably from our estimate of 29 kJ/mol; this might in fact be due to an oversimplified kinetic model used from these authors⁸ accounting for a pure irreversible isomerization mechanism.

An issue that merits further discussion is why the present isomerization is nearly isoenergetic in the first excited state S_1 but differs noticeably in energy in the ground state S_0 . The equilibrium geometry of each rotamer, in both electronic states S_0 and S_1 , should to a large extent be determined by (a) the overlap between the sp^2 hybridized oxygen lone pair with the orbitals of the naphthalene ring and (b) the steric repulsion between methyl group hydrogen atoms and the close lying hydrogen atom attached to the naphthalene subunit. It is generally accepted that simple aromatic molecules possessing a single bond that joins two conjugated groups show the tendency to adopt planar configurations.²⁴ The driving force toward planarity is the resonance between the conjugated groups;²⁵ this resonance interaction is much more pronounced

in the S_1 state. As proven by X-ray crystallography¹⁶ and supported by quantum mechanical calculations,^{9b} the *s-cis* rotamer (syn, $\varphi = 0^\circ$) of the present compound **1** is the more stable form in the ground state S_0 . A value of 1.374 Å is found from X-ray¹⁶ (1.347 Å from theory^{9b}) for the $\text{C}_2\text{-O}_{11}$ bond length which connects the methoxy group to the naphthalene subunit. This value is significantly shorter than a typical single C–O bond length (1.43 Å in methyl ether²⁶), indicating a substantial double-bond character of the $\text{C}_2\text{-O}_{11}$ linking. Furthermore the angle $\text{C}_2\text{-O}_{11}\text{-CH}_3$ is found to be 117.22° from X-ray¹⁶ (119.5° from theory^{9b}), demonstrating that the oxygen atom exhibits considerable sp^2 character in the ground state. In S_1 it is expected, by analogy to similar systems,²⁵ that the resonance interaction between the sp^2 hybridized oxygen lone pair and naphthalene orbitals be more effective. The latter is further supported by theoretical methods^{9b} where (a) a shortening of the $\text{C}_2\text{-O}_{11}$ bond, albeit weak ($\sim 0.01 \text{ Å}$), is calculated and (b) a noticeable relief of the $\text{C}_1\text{-C}_2\text{-O}_{11}$ angle strain toward the unperturbed one ($\sim 120^\circ$) is found in S_1 relative to that in the ground state (122.7° in S_1 and 125.5° in S_0 ; 125.9° from X-ray¹⁶). The above data strongly suggest that in the *s-cis** form the oxygen atom should be (a) almost perfectly planarized and (b) strainlessly attached to the aromatic ring. Therefore one might expect the excitation delocalization to be equally distributed on the naphthalene ring at the equilibrium geometry of each rotamer in S_1 (*planar forms* $\varphi = 0^\circ$, $\varphi = 180^\circ$). Furthermore intramolecular steric hindrance, between methyl group hydrogen atoms and the close lying hydrogen atom attached to the aromatic ring, should be effectively balanced in both rotamers in S_1 . This is because the carbon atom of the methoxy group retains, to a large extent, its sp^3 character^{9b} in S_1 , and consequently, restricted rotation about the O–CH₃ axis may sufficiently moderate the above steric interactions. Therefore, in the first excited state S_1 , the interplay between intramolecular steric hindrance and electronic interactions in both configurations (*s-cis** and *s-trans**) should be sufficiently balanced to give nearly degenerate energetic levels. The above steric relief appears not to be effective for other compounds that undergo *s-cis** to *s-trans** interconversion such as 2-vinylnaphthalene^{1b} and other vinyl derivatives.⁷ A plausible explanation given also in the literature is that the fixed vinyl hydrogens are exposed to more severe and unequal periplanar repulsions at the equilibrium geometry of each rotamer.^{1b}

In the ground state S_0 there is sufficient evidence that steric interaction predominantly accounts for the observed difference in energy between the two rotational isomers of **1**. It is well studied that 2-hydroxynaphthalene (2-HN) exists in a supersonic jet in *s-cis* and *s-trans* conformations arising from distinguishable orientations of the hydroxy group.^{9c} The two electronic origins of 2-HN are separated by 317 cm^{-1} . If the hydrogen atom of the hydroxy group is replaced by a methyl group (2-methoxynaphthalene), the above energy separation is duplicated ($\sim 660 \text{ cm}^{-1}$).^{9a} Such a large difference in energy, after exocyclic substitution, is unlikely to arise primarily from a shift in the excited-state energies as clearly demonstrated in this work. Therefore a steric effect is undoubtedly present in the ground state and could successfully explain the observed energy difference of the two rotational isomers. The presence of steric

(23) Reaction enthalpy: $\Delta H^{\text{S}_1} = E_a^{-1} - E_a^1 \cong 0.3 \text{ kJ/mol}$. Free reaction enthalpy: $\Delta G_{(T)}^{\text{S}_1} = -RT \ln(k_{1(T)}/k_{-1(T)})$. Reaction entropy: $\Delta S^{\text{S}_1} = R \ln(k_{1(T)}^{\text{S}_1}/k_{-1(T)}^{\text{S}_1}) = R \ln(k_{1(T)}^0/k_{-1(T)}^0) \cong 2 \text{ J}\cdot\text{K}^{-1}\cdot\text{mol}^{-1}$. $k_{1(T)}^0 = (2.15 \pm 0.5) \times 10^{13} \text{ s}^{-1}$ and $k_{-1(T)}^0 = (1.6 \pm 0.5) \times 10^{13} \text{ s}^{-1}$ are frequency factors for the forward and reverse reaction, respectively, obtained from Arrhenius plots in Figure 3.

(24) (a) Werst, D. W.; Brearley, A. M.; Gentry, W. R.; Barbara, P. F. *J. Am. Chem. Soc.* **1987**, *109*, 32. (b) Muszkat, K. A.; Wismontski-Knittel, T. *Chem. Phys. Lett.* **1981**, *83*, 87. (c) Muszkat, K. A.; Wismontski-Knittel, T. *J. Phys. Chem.* **1981**, *85*, 3427.

(25) (a) Amlöf, J. *Chem. Phys.* **1974**, *6*, 153. (b) Birner, P.; Hoffman, H. J. *Int. J. Quantum Chem.* **1982**, *21*, 833. (c) Carter, R. E.; Liljefors, T. *Tetrahedron* **1976**, *32*, 2915. (d) Warshel, A.; Karplus, M. *J. Am. Chem. Soc.* **1972**, *21*, 5612.

(26) *Handbook of Chemistry and Physics*, 70th ed.; CRC Press: Boca Raton, FL, 1989.

hindrance in S_0 is also supported from theoretical methods in the case of the *s-cis* form^{9b} of **1** and of the simpler analogue methoxybenzene.²⁷ Most likely, contrary to S_1 , electronic and steric asymmetric interactions induced by a distorted sp^2 hybridized oxygen atom might in principle be responsible for the observed energy gap between the two rotamers in S_0 .

Finally it is interesting to note that, if one combines the energy separation of the two electronic origin transitions of the two rotamers experimentally obtained from gas-phase vibronic spectroscopy^{9a} (660 cm^{-1}) with their ground state energy gap calculated from an *ab initio* study^{9b} (the *s-trans* form lies $\sim 700\text{ cm}^{-1}$ higher in energy than the *s-cis* analogue), then one indirectly obtains an estimation of only $\sim 40\text{ cm}^{-1}$ ($\sim 0.5\text{ kJ/mol}$) for the energy gap between the two rotamers in S_1 . That is, the two rotamers are nearly isoenergetic in S_1 supporting

thus our conclusions in the present work reached by straightforward kinetic analysis.

4. Conclusions

The results from this work provide the first detailed insights into the *high reversibility* of an excited-state rotameric equilibration in solution. Our findings clearly demonstrate that, above 260 K, *s-cis** and *s-trans** rotational isomers of 2-methoxynaphthalene interconvert through very close lying energy barriers with respect to the *forward* and *reverse* isomerization pathway. This leads to an excited-state equilibrium constant very close to 1, which is not noticeably affected over the temperature region studied. To the best of our knowledge, in contrast to the generally accepted photodynamic scheme of related compounds, this is the first experimental manifestation of a nearly fully reversible torsional photoisomerization in solution.

JA074638N

(27) (a) Vincent, M. A.; Hillier, I. H. *Chem. Phys.* **1990**, *140*, 35. (b) Spellmeyer, D. C.; Grootenhuis, P. D. J.; Miller, M. D.; Kuyper, L. F.; Kollman, P. A. *J. Phys. Chem.* **1990**, *94*, 4483.